scientific reports

Check for updates

OPEN

PFKFB3 ameliorates ischemia-induced neuronal damage by reducing reactive oxygen species and inhibiting nuclear translocation of Cdk5

Hyun Jung Kwon[1,2], Kyu Ri Hahn[3], Seung Myung Moon[4,5], Dae Young Yoo[3], Dae Won Kim[1]✉ & In Koo Hwang[3]✉

The enzyme 6-phosphofructo-2-kinase/fructose-2,6-bisphosphatase (PFKFB) plays an essential role in glycolysis and in the antioxidant pathway associated with glutathione. Therefore, we investigated the effects of PFKFB3 on oxidative and ischemic damage. We synthesized a fusion protein of transactivator of transcription (Tat)-PFKFB3 to facilitate its passage into the intracellular space and examine its effects against oxidative stress induced by hydrogen peroxide (H_2O_2) treatment and ischemic damage caused by occlusion of the common carotid arteries for 5 min in gerbils. The Tat-PFKFB3 protein was efficiently delivered into HT22 cells in a concentration- and time-dependent manner, with higher levels observed 18 h after treatment. Furthermore, treatment with 6 μM Tat-PFKFB3 demonstrated intracellular delivery into HT22 cells, as analyzed through immunocytochemical staining. Moreover, it significantly ameliorated the reduction of cell viability induced by 200 μM H_2O_2 treatment. Tat-PFKFB3 treatment also alleviated H_2O_2-induced DNA fragmentation and reactive oxygen species formation in HT22 cells. In gerbils, the intraperitoneal administration of 2 mg/kg Tat-PFKFB3 efficiently delivered the substance to all hippocampal areas, including the hippocampal CA1 region. This administration significantly mitigated ischemia-induced hyperlocomotion, long-term memory deficits, and ischemic neuronal death in the hippocampal CA1 region after ischemia. Additionally, treatment with 2 mg/kg Tat-PFKFB3 significantly ameliorated the translocation of Cdk5 from the cytosol to the nucleus in the hippocampal CA1 region 24 h after ischemia, but not in other regions. The treatment also significantly reduced reactive oxygen species formation in the CA1 region. These findings suggest that Tat-PFKFB3 reduces neuronal damage in the hippocampal CA1 region after ischemia through the reduction of Cdk5 signaling and reactive oxygen species formation. Therefore, Tat-PFKFB3 may have potential applications in reducing ischemic damage.

Keywords PFKFB3, Oxidative stress, Ischemia, Cdk5, Nuclear translocation

Transient forebrain ischemia is characterized by an insufficient supply of oxygen and glucose to the brain, which causes selective neuronal damage due to high oxygen consumption and low antioxidative potential[1]. The brain utilizes glucose as the main fuel source and synthesizes ATPs via glycolysis and oxidative phosphorylation[1]. Most of the energy is produced in the mitochondria via the cooperative activity of the respiratory chain and metabolic enzymes. However, in the ischemic state, temporary or permanent disruption of blood flow impairs energy metabolism in the brain[2,3] and sharply decreases ATP production. In addition, the post-ischemic brain shows

[1]Department of Biochemistry and Molecular Biology, Research Institute of Oral Sciences, College of Dentistry, Gangneung-Wonju National University, Gangneung 25457, South Korea. [2]Department of Biomedical Sciences, Research Institute for Bioscience and Biotechnology, Hallym University, Chuncheon 24252, South Korea. [3]Department of Anatomy and Cell Biology, College of Veterinary Medicine, Research Institute for Veterinary Science, Seoul National University, Seoul 08826, South Korea. [4]Department of Neurosurgery, Kangnam Sacred Heart Hospital, College of Medicine, Hallym University, Seoul 07441, South Korea. [5]Research Institute for Complementary & Alternative Medicine, Hallym University, Chuncheon 24253, South Korea. ✉email: kimdw@gwnu.ac.kr; vetmed2@snu.ac.kr

reduced glucose oxidation[4]. Moreover, energy-dependent processes are closely related to the vulnerability of the brain to ischemic damage[5]. Reperfusion produces abundant reactive oxygen species (ROS) and subsequently activates neuroinflammatory cascades in several brain regions[6]. Mongolian gerbils (*Meriones unguiculatus)* are widely used as an animal model for forebrain ischemia because of their low mortality and technical convenience compared to rats or mice[7]. In addition, whole genome sequencing and clustered regularly interspaced short palindromic repeats (CRISPR)/CRISPR-associated protein 9 (Cas9) technology facilitates the usage of gerbils as a model for cerebral ischemia[8,9]. Transient forebrain ischemia in Mongolian gerbils causes selective neuronal damage to the hippocampus, neocortex, and thalamus[10–12]. In particular, the recovery of the mitochondrial redox ratio is delayed in the hippocampal CA1 region in the early and late periods after ischemia in gerbils[13].

The enzyme 6-phosphofructo-2-kinase/fructose-2,6-bisphosphatase (PFKFB) is critical for glucose metabolism. The PFKFB family consists of four isozymes, PFKFB1–4[14], of which PFKFB3 is ubiquitously expressed in various tissues, including the brain[15,16]. In the normal brain, PFKFB3 is highly expressed in astrocytes but has very low expression in neurons[16] because it is degraded by the E3 ubiquitin ligase anaphase-promoting complex/cyclosome (APC/C-Cdh1)[17,18]. Therefore, low levels of PFKFB3 facilitate the pentose–phosphate pathway (PPP)-mediated antioxidant pathway to maintain glutathione (GSH) and scavenge ROS by generating reduced nicotinamide adenine dinucleotide phosphate[19]. However, excitotoxic conditions, via the activation of glutamate receptors, stabilize PFKFB3 by inhibiting APC/C-Cdh1 via cyclin-dependent kinase-5 (Cdk5)-p25[20], decreasing PPP, and eventually causing neuronal death[21,22]. Moreover, oxygen-glucose deprivation increases PFKFB3 expression in primary neurons 12 h after an insult[23]. Glycolysis is required for normal function in the hippocampus[24] and is enhanced after cerebral ischemia[25].

Recently, there have been controversial findings regarding the effects of PFKFB3 inhibition on various diseases. Both pharmacological and genetic inhibition of PFKFB3 have been found to protect neurons from ischemic damage[26,27]. In contrast, PFKFB3 inhibition has been found to aggravate spinal cord injury-induced neuronal damage[28] and reduce the cardioprotective effects against ischemic myocardial injury[29]. However, activating PFKFB3 with meclizine has been shown to alleviate neurological impairments induced by spinal cord injury[28]. The expression of PFKFB3 in microvessels is markedly lower in the aged brain compared to younger ones[30]. Overexpression of PFKFB3 improves the reduction in contractile function and blood flow in the limb caused by ischemia[31]. Recent studies have demonstrated the protective effects of PFKFB3 against oxidative stress in diabetic animals and its ability to reduce ROS production in diabetic cardiomyocytes[32]. Therefore, it is worth investigating the effects of PFKFB3 on oxidative and ischemic damage.

The brain has a self-protective structure between the bloodstream and brain tissue known as the blood–brain barrier (BBB), which protects it from circulating ions, toxins, inflammation, and pathogens[33]. However, the BBB can hinder the treatment of brain diseases because drugs cannot cross it. Transactivator of transcription (Tat), a cell-penetrating peptide derived from the human immunodeficiency virus, can transport various cargos across the BBB[34]. In previous studies, the Tat-cargo fusion protein was successfully delivered to the hippocampus[35,36] after ischemia, even when the BBB was compromised[37,38].

The focal ischemic model induced by the occlusion of the middle cerebral artery is believed to cause severe brain damage and oxygen-glucose deprivation and is considered to be a comparable in vitro model. In contrast, neuronal damage in transient forebrain ischemia is not as severe compared to a model in which focal ischemia and oxidative stress are induced by hydrogen peroxide (H_2O_2), which exhibits similar phenotypes to transient forebrain ischemia. Therefore, in the present study, we aimed to synthesize a Tat-PFKFB3 protein for efficient delivery into hippocampal neurons and examine its effects on PFKFB3 oxidative stress in HT22 cells and ischemia/reperfusion damage in the gerbil hippocampus.

Materials and methods

Synthesis of Tat-PFKFB3 and its control protein. The pET15b vector system was used to express the Tat-PFKFB3 recombinant protein in *Escherichia coli* BL21 cells (Novagen), with the insertion of human PFKFB3 cDNA, 6X histidine (His), and the Tat peptide, as previously described[35,36]. Briefly, transformed cells with Tat-PFKFB3 or the control (PFKFB3) plasmids were cultivated, and the proteins were overexpressed. After elution, the proteins were purified using a Ni^{2+}-nitrilotriacetic acid Sepharose affinity column (Qiagen, Valencia, CA, USA) and PD-10 column chromatography. The presence of the His-tag was confirmed by western blotting to detect the 6X His, as previously described[35,36].

Confirmation of Tat-PFKFB3 delivery in HT22 cells. Western blotting and immunofluorescent staining for His-tags were performed to confirm the delivery of Tat-PFKFB3 protein into HT22 cells. The HT22 cells from the mouse hippocampus were grown as previously described[35,36] and were incubated with various concentrations of Tat-PFKFB3 and PFKFB3 (0 to 8.0 μM) for 60 min. In addition, 6.0 μM protein was added to HT22 cells at various time points (0 to 60 min). To assess the degradation of Tat-PFKFB3 protein, the 6.0 μM protein was incubated for 42 h after protein treatment. The protein expressions were confirmed by western blotting with mouse anti-His-tag (1:1,000; Abcam, Cambridge, UK) or mouse anti-β-actin (1:5,000; Cell Signaling, Danvers, MA, USA), and peroxidase-conjugated anti-mouse IgG (1:1,000; Abcam), as previously described[35,36].

To visualize the delivered proteins, HT22 cells were grown on coverslips and incubated with 6.0 μM Tat-PFKFB3 and PFKFB3 for 60 min. Cells were fixed with 4% paraformaldehyde at 25°C for 5 min and were sequentially incubated with mouse anti-His-tag (1:1,000; Abcam) and Alexa 488-conjugated anti-mouse IgG (1:500; Jackson ImmunoResearch Inc., West Grove, PA, USA) with 1 μg/mL 4′,6-diamidino-2-phenylindole (Roche Applied Science, Mannheim, Germany), as previously described[35,36].

Neuroprotective effects of Tat-PFKFB3 against oxidative stress in HT22 cells. Various concentrations of Tat-PFKFB3 or PFKFB3 proteins were exposed to HT22 cells for 1 h, along with oxidative stress induced by 200 μM hydrogen peroxide (H_2O_2). Thereafter, the cells were harvested to assess the cytotoxicity using a water-soluble tetrazolium salt (WST-1) assay kit, according to the manufacturer's guidelines to find the optimal concentration,

as previously described[35,36]. In addition, 6.0 μM PFKFB3 and Tat-PFKFB3 were incubated for 60 min with 200 μM H_2O_2, followed by incubation with 1 μM 5-carboxyfluorescein diacetate acetoxymethyl ester (5-CFDA AM) (Invitrogen, Carlsbad, CA, USA) and 1 μg/mL DAPI (Roche Applied Science) for 15 min at 37 °C.

ROS formation and DNA fragmentation were assessed in coverslip-cultured HT22 cells 1 h after incubation with 6.0 μM PFKFB3 or Tat-PFKFB3 and 200 H_2O_2. ROS formation and DNA fragmentation were visualized by staining with 2,7-dichlorofluorescein diacetate (DCF-DA) and terminal deoxynucleotidyl transferase-mediated deoxyuridine triphosphate-biotin nick end labeling (TUNEL), combined with 1 μg/mL DAPI (Roche Applied Science), respectively, as previously described[35,36].

Experimental animals and ischemic surgery. Mongolian gerbils (male, 6 weeks old) were purchased from Japan SLC Inc. (Shizuoka, Japan) and acclimatized for 2 weeks. All animal experiments were conducted in accordance with the ARRIVE guidelines, and the protocols were approved by the Institutional Animal Care and Use Committee of Seoul National University (Approval number: SNU-200313-2-5). The experiments were performed in accordance with relevant guidelines and regulations from the committee. Gerbils (male, 1 year old) were randomly divided into the following six groups: (1) control (normal gerbils), (2) vehicle (10% glycerol), (3) Tat peptide, (4) 2.0 mg/kg PFKFB3, (5) 0.5 mg/kg, and (6) 2.0 mg/kg Tat-PFKFB3.

Anesthesia was induced using 2.5% isoflurane (Baxter, Deerfield, IL, USA) mixed with nitrogen and oxygen. A 5-minute occlusion was performed using aneurysm clips to induce ischemic damage, and vehicle, Tat peptide, PFKFB3, or Tat-PFKFB3 were intraperitoneally administered only once to the gerbils immediately after reperfusion. The intraperitoneal route was chosen because it causes minimal stress in animals and is considered suitable for pharmacological and proof-of-concept studies[39].

Behavioral assessment. One day after ischemia/reperfusion, spontaneous motor activity was recorded for 60 min in a soundproof plexiglass cage (25 cm × 20 cm × 12 cm) using a digital camera (Basler, Ahrensburg, Germany). Motor activity was assessed based on the time consumed in the mobile phase and the total distance traveled using the XT14 software (Ethovision, Wageningen, The Netherlands).

Six days after ischemia, training trial was performed by placing each gerbil in the light compartment to explore the compartment after opening the sliding gate. Seven days after ischemia/reperfusion, the testing trial was performed to assess long-term memory in gerbils after ischemic damage. The animal was placed in the light compartment and the latent time period to enter the dark compartment was recorded.

Immunohistochemical staining. Two hours, four, or ten days after ischemia/reperfusion, animals were sacrificed with isoflurane anesthesia and perfused with 0.01 M phosphate-buffered saline (PBS) and 4% paraformaldehyde. The brain was removed immediately and fixed with the same fixative for 12 h and stored in 30% sucrose until it sank. Thirty micrometer tissue sections were made based on the gerbil brain atlas, 1.4–2.0 mm caudal to the bregma[40], using a sliding microtome with a freezing stage (HM430, Thermo Fisher Scientific, Waltham, MA, USA). Five Sect. (120 μm interval in each section) per animal were incubated with rabbit anti-His-tag (1:1000, Novus Biologicals, Centennial, CO, USA) and mouse anti-neuronal nuclei (NeuN) antibody (1:1000; EMD Millipore, Temecula, CA, USA) at 4 °C for 48 h to visualize the delivered PFKFB3 proteins and surviving neurons, respectively. Sections were incubated with Cy3-conjugated goat anti-rabbit IgG (1:500, Jackson ImmunoResearch Inc.) or goat anti-mouse IgG (1:200; Vector Laboratories, Burlingame, CA, USA) and peroxidase-conjugated streptavidin (1:200; Vector Laboratories) at 25 °C for 2 h. Thereafter, sections were incubated with 0.05% 3,3-diaminobenzidine tetrahydrochloride (Sigma-Aldrich, St. Louis, MO, USA) in 0.01 M PBS to develop the immunoreactive signals.

Double immunofluorescent staining. To examine the expression of transduced Tat-PFKFB3 proteins in astrocytes and microglia, double immunofluorescent staining was performed in the hippocampal CA1 region using His-tag and glial markers. Five sections per animal were incubated with rabbit anti-His-tag (1:1000, Novus Biologicals) and either mouse anti-glial fibrillary acidic protein (GFAP) antibody (1:1000; EMD Millipore) or goat anti-ionized calcium-binding adaptor molecule 1 (Iba1) antibody (1:500, Novus Biologicals) at 4 °C for 3 days. Afterwards, the sections were incubated with Cy3-conjugated donkey anti-rabbit IgG (1:500, Jackson ImmunoResearch Inc.) and either FITC-conjugated donkey anti-rabbit IgG (1:500, Jackson ImmunoResearch Inc.) or FITC-conjugated donkey anti-goat IgG (1:500, Jackson ImmunoResearch Inc.) at 25 °C for 2 h.

Effects of Tat-PFKFB3 on Cdk5 expression against transient forebrain ischemia in gerbils. Cdk5 expression was assessed 24 h after ischemia to address the neuroprotective mechanisms of Tat-PFKFB3 against ischemic damage in the hippocampus. Animals in each group were re-anesthetized with isoflurane immediately after measuring spontaneous motor activity, hippocampal tissues were collected with 30-μm coronal sections as described above, and immunohistochemical staining for Cdk5 was performed. Briefly, the following primary antibodies were used: mouse anti-Cdk5 antibody (1:200; Santa Cruz Biotechnology Inc., Santa Cruz, CA, USA), goat anti-mouse IgG (1:200; Vector Laboratories), and peroxidase-conjugated streptavidin (1:200; Vector Laboratories).

In addition, Cdk5 protein levels in the hippocampal CA1 region were assessed using western blotting. The animals in each group were re-anesthetized with isoflurane 24 h after ischemia and the hippocampal tissues were obtained with 500-μm coronal section using a vibratome (Leica, Wetzlar, Germany). The hippocampal CA1 region was dissected, homogenized, and the nuclear fraction of proteins was obtained. The fractionated protein was then loaded onto an SDS-PAGE gel, transferred onto a nitrocellulose membrane (Pall Crop, East Hills, NY, USA), and incubated with the following antibodies: mouse anti-Cdk5 (1:1000; Santa Cruz Biotechnology Inc.), rabbit anti-laminin B (1:1,000; Abcam), mouse anti-glyceraldehyde-3-phosphate dehydrogenase (GAPDH, 1:5,000; Abcam), and mouse β-actin (1:5,000; Cell Signaling). Subsequently, the protein bands were developed using chemiluminescent reagents after incubation with peroxidase-conjugated anti-mouse IgG (1:1,000; Abcam) or anti-rabbit IgG (1:1,000; Abcam).

Visualization of ROS in the hippocampal CA1 region. Animals were sacrificed 24 h after ischemia to visualize the intracellular ROS in the hippocampal CA1 region. Briefly, animals were euthanized with isoflurane,

and the brain tissues were quickly dissected from the skull. Thirty-micrometer tissue sections were made based on the gerbil brain atlas, 1.4–2.0 mm caudal to the bregma[40], using a vibratome (VT1000M, Leica) without any fixation. The sections were incubated with a 5 μM dihydroethidium (DHE) solution at 25 °C for 20 min, and then coverslipped with a DPX mounting medium after washing, as described in a previous study[41].

Data analysis. Immunohistochemical results were quantified using the ImageJ software version 1.53f51 (National Institutes of Health, Bethesda, MD, USA). Five sections per animal were stained with NeuN, and the number of NeuN-immunoreactive neurons was counted in the hippocampal CA1 region, while others were quantified as the optical density of the immunoreactive or DHE-stained structure (sum of pixel number × gray scale). The calculated values in each section were averaged per animal and normalized to the percentile values of the control group.

The percentile data are shown as the mean ± standard deviation, and the data were statistically analyzed using GraphPad Prism 5.01 software (GraphPad Software Inc., La Jolla, CA, USA). Between-group comparison was performed using Student's *t*-test and one-way analysis of variance, followed by Tukey's multiple comparison *post hoc* test. The statistical significance level was set at $p < 0.05$.

Results

Validation of synthesized Tat-PFKFB3 and PFKFB3 protein delivery in HT22 cells. Overexpressed and purified Tat-PFKFB3 and PFKFB3 proteins with 6X His were assessed using Coomassie brilliant blue staining and western blotting for His-tags. Coomassie brilliant blue staining revealed various protein bands. Strong bands were detected at approximately 58 and 60 kDa, which were identified as PFKFB3 and Tat-PFKFB3, respectively (Fig. 1A).

PFKFB3 and Tat-PFKFB3 proteins were incubated at various concentrations and time points to assess the protein delivery. As expected, the control and PFKFB3-treated groups did not show His-tag bands at any concentration or incubation time, whereas treatment with Tat-PFKFB3 significantly increased His-tag expression in a concentration- and time-dependent manner. The protein expression level was more than 10-fold for 4–8 μM Tat-PFKFB3 treatment for 1 h or incubation time longer than 45 min (Fig. 1B and C).

Degradation of the intracellularly delivered Tat-PFKFB3 protein was observed at 42 h after protein treatment. The protein expression level gradually decreased with time after treatment and demonstrated significantly higher levels 18 h after treatment; thereafter, there were no significant differences compared to the control group (Fig. 1D).

Intracellularly delivered protein localization was visualized via immunocytochemical staining for His-tag in HT22 cells. His-tag immunoreactivity was not detected in the control and PFKFB3-treated HT22 cells, whereas it was abundant in the cytoplasm of Tat-PFKFB3-treated cells (Fig. 1E).

Neuroprotective effects of Tat-PFKFB3 and PFKFB3 proteins on H_2O_2-induced oxidative damage in HT22 cells. HT22 cells were simultaneously exposed to 200 μM H_2O_2 and Tat-PFKFB3 or PFKFB3 for 1 h to detect the neuroprotective effects of the proteins at various concentrations using the WST-1 assay. Vehicle-treated HT22 cells showed a significantly lower (51.8%) cell viability than the control group, and treatment with PFKFB3 did not result in significant changes in cell viability at any concentration. However, incubation with Tat-PFKFB3 increased the viability of HT22 cells in a concentration-dependent manner and resulted in significantly higher cell viability levels (71.2 and 88.8% of the control, respectively) at 6 and 8 μM protein concentrations (Fig. 2A). We set the optimal concentration of Tat-PFKFB3 at 6 μM because it was the minimal concentration to show significant improvement in cell viability.

Surviving cells were visualized via staining for 5-CFDA AM in HT22 cells after simultaneous exposure to 200 μM H_2O_2 and 6 μM Tat-PFKFB3 or PFKFB3 for 1 h. In the control group, several cells were stained with 5-CFDA AM. However, very few 5-CFDA AM-stained cells were observed in the vehicle- or PFKFB3-treated groups and demonstrated significantly lower fluorescence intensity (21.4% and 21.9%, respectively) than the control group. In the Tat-PFKFB3-treated group, numerous cells were stained with 5-CFDA AM, and the decrease in fluorescence intensity was significantly ameliorated (75.2% of the control) (Fig. 2B).

DCF-DA and TUNEL staining were performed to visualize the effects of 6 μM Tat-PFKFB3 or PFKFB3 against 200 μM H_2O_2-induced ROS formation and DNA fragmentation in HT22 cells. In the control group, DCF and TUNEL fluorescence were nearly absent in HT22 cells. However, in vehicle- and PFKFB3-treated groups, DCF- and TUNEL-stained structures were abundantly found in the cells. In these groups, the fluorescence intensity of DCF and TUNEL was observed to be between 601.8% and 770.9% of that of the control group. In addition, in the Tat-PFKFB3-treated group, a few cells were stained with DCF and TUNEL and showed significantly lower levels (204.5% and 289.7%, respectively) of fluorescence intensity than their respective control groups (Fig. 2C and D).

Validation of synthesized Tat-PFKFB3 and PFKFB3 protein delivery in gerbil hippocampus. Two hours after ischemia/reperfusion, the delivered PFKFB3 was visualized via immunohistochemical staining for His-tag in the brain because 6X His was inserted in the pET15b vector system to detect the exogenous PFKFB3 protein. In the vehicle- and Tat peptide-treated groups, no His-tag immunoreactive structures were detected in the hippocampal CA1 region. In the 2.0 mg/kg PFKFB3-treated group, little His-tag immunoreactivity was found in the CA1 region, but did not show any significant changes between the control and 2.0 mg/kg PFKFB3-treated groups. In the 0.5 and 2.0 mg/kg Tat-PFKFB3-treated groups, His-tag immunoreactive structures were found in the CA1 region and His-tag immunoreactivity was significantly increased to 202.2% and 252.6% of the vehicle-treated group, respectively (Fig. 3A). In the 2.0 mg/kg Tat-PFKFB3-treated group, His-tag immunoreactivity was observed in all hippocampal subregions, including the CA1-3 region and dentate gyrus (Fig. 3A).

Within the hippocampal CA1 region, His-tag immunoreactivity was abundantly found in the pyramidal cells in stratum pyramidale, while a small number of non-neuronal cells exhibited His-tag immunoreactivity. In order to examine the expression of His-tag in glial components, double fluorescent staining for His-tag and

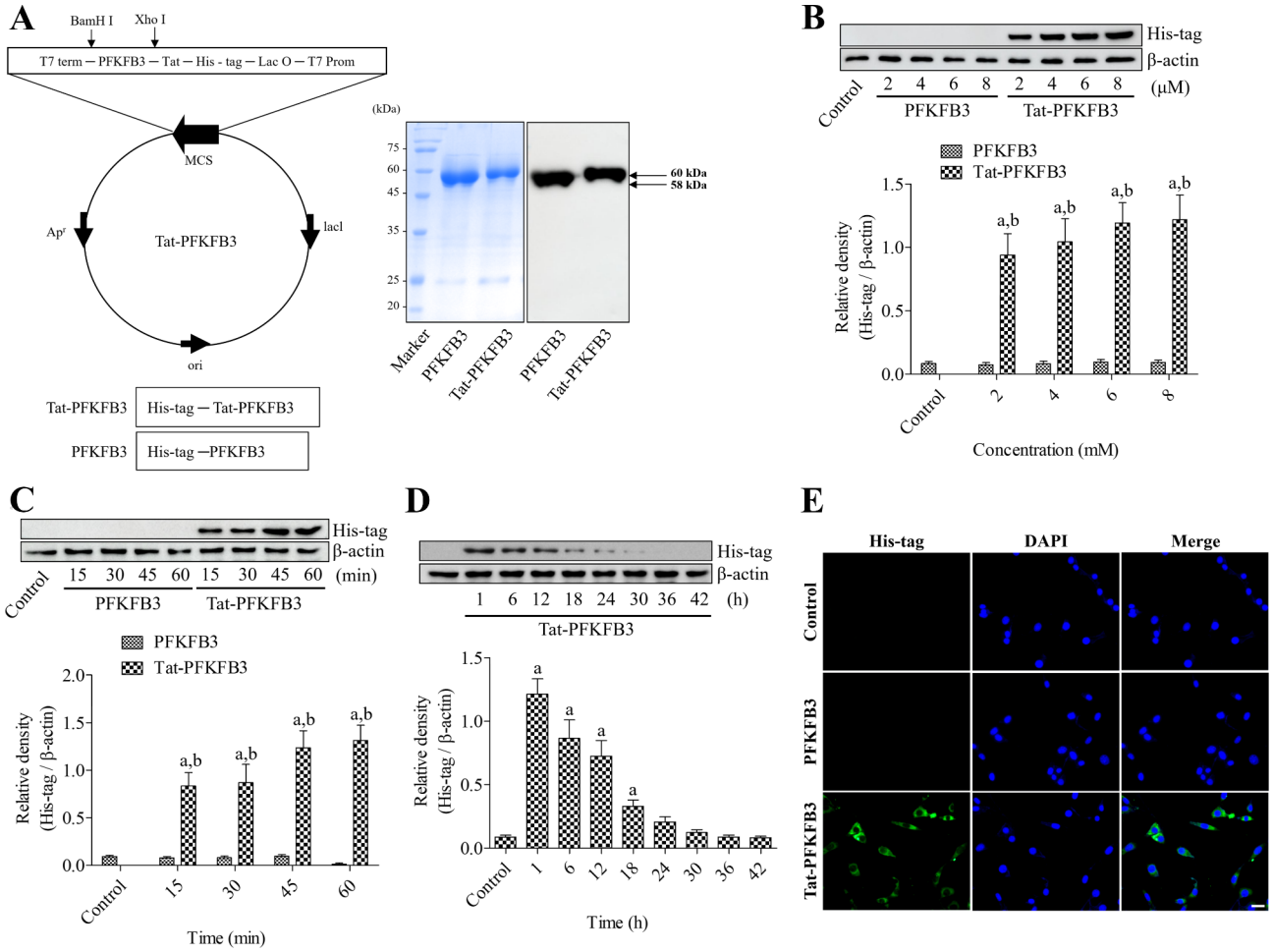

Fig. 1. Validation of synthesized Tat-PFKFB3 and PFKFB3 protein delivery in HT22 cells. (A) Tat-PFKFB3 and its control protein (PFKFB3) were designed based on the pET15b vector system with 6X His and PFKFB3 with/without the Tat expression vector, respectively. Transformation to cells, cultivation, induction, purification, and protein expression were validated by Coomassie brilliant blue staining and western blotting for His-tag. (B) Purified proteins were incubated for 60 min in HT22 cells to confirm the concentration-dependent delivery of protein. (C) The proteins (6.0 μM) were added at various time points to assess the time-dependent delivery of protein. (D) The proteins (6.0 μM) were added for longer times to assess protein degradation. (B-D) The delivered proteins were validated via western blotting for His-tag, and all assays were performed in triplicate. Data are shown as mean ± standard deviation, and the differences were analyzed using Student's *t*-test (B and C) and one-way analysis of variance followed by Tukey's multiple comparison *post hoc* test (D) ($n = 5$, $^{a}p < 0.05$, significantly different from the control group; $^{b}p < 0.05$, significantly different from the 60 min group). (E) The proteins (6.0 μM) were added for 60 min and immunochemical staining for His-tag was performed to visualize the delivered proteins in HT22 cells. Scale bar = 20 μm.

GFAP or Iba-1 was conducted. Several GFAP-immunoreactive astrocytes and Iba1-immunoreactive microglia were found to colocalize with His-tag in the CA1 region (Fig. 3B).

Neuroprotective effects of Tat-PFKFB3 and PFKFB3 proteins on ischemia-induced neuronal damage in gerbils. One day after ischemia/reperfusion, spontaneous motor activity was observed to assess the distance traveled because ischemia-induced hyperactivity is caused by functional impairments in the hippocampus. Gerbils in the vehicle-treated group traveled significantly longer (268.0%) than those in the control group. In the Tat peptide- and 2.0 mg/kg PFKFB3-treated groups, the traveled distance was similar to that of the vehicle-treated group. In the 0.5 and 2.0 mg/kg Tat-PFKFB3-treated groups, the gerbils traveled shorter distances in a concentration-dependent manner; however, a significant mitigation of distance traveled (121.1% of control) was only found in the 2.0 mg/kg Tat-PFKFB3-treated group compared to the vehicle-, Tat peptide-, and 2.0 mg/kg PFKFB3-treated groups (Fig. 4A).

Six and seven days after ischemia/reperfusion, memory deficits were assessed via training and test sessions of the passive avoidance test. In the vehicle- and Tat peptide-treated groups, the latency was significantly decreased to 31.6% and 25.8% of the control group, respectively. In the 2.0 mg/kg PFKFB3-treated group, the latency was similar to that in the vehicle-treated group. However, in the 0.5 and 2.0 mg/kg Tat-PFKFB3-treated groups, the

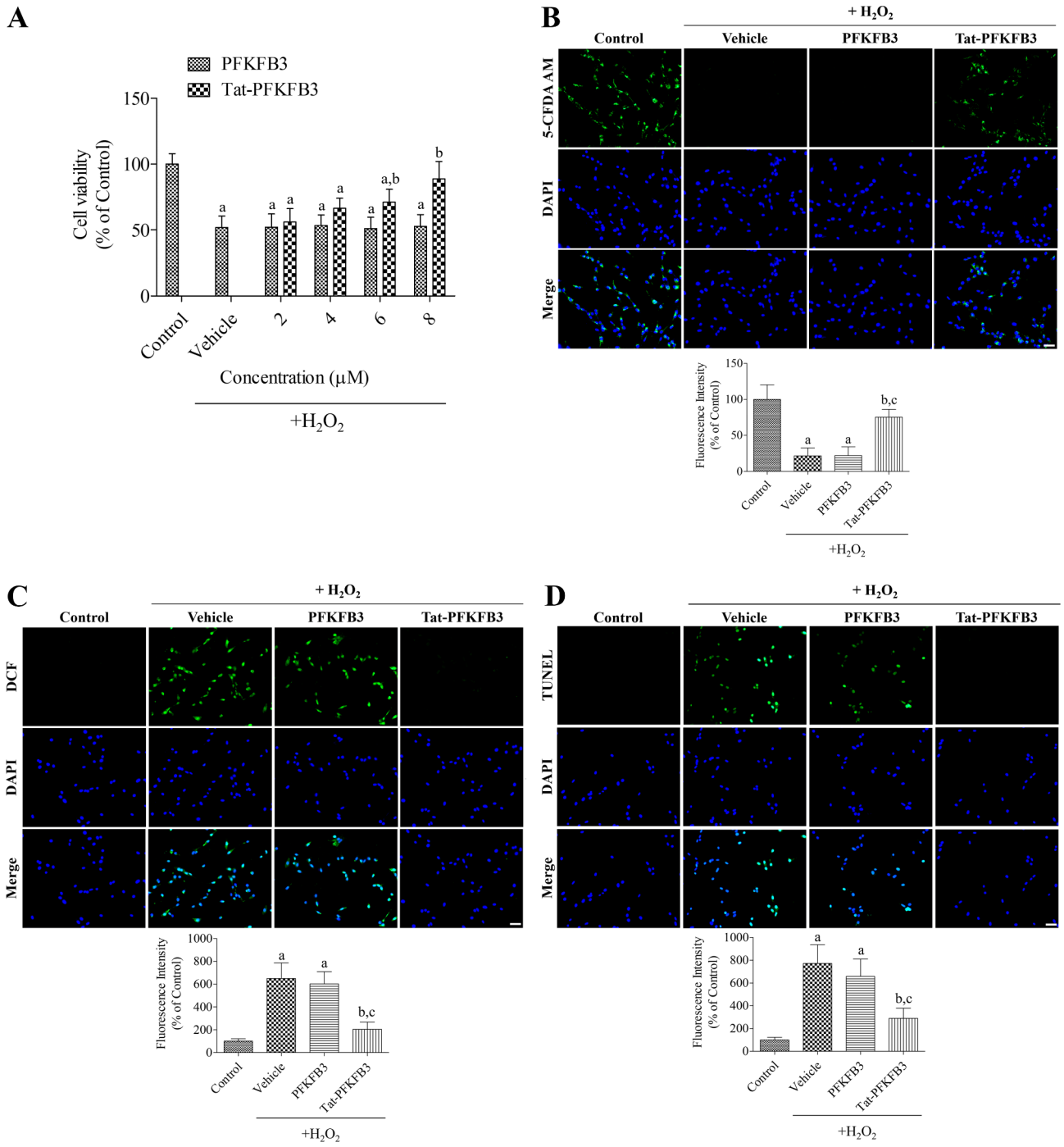

Fig. 2. Neuroprotective effects of Tat-PFKFB3 and PFKFB3 proteins on H_2O_2-induced oxidative damage in HT22 cells. (A) Purified proteins and 200 μM H_2O_2 were incubated for 60 min in HT22 cells to determine the optimal concentration showing neuroprotective effects of proteins. (B–D) The proteins (6.0 μM) and 200 μM H_2O_2 were incubated for 60 min and 5-carboxyfluorescein diacetate acetoxymethyl ester (5-CFDA AM), 2,7-dichlorofluorescein diacetate (DCF-DA), and deoxynucleotidyl transferase-mediated deoxyuridine triphosphate-biotin nick end labeling (TUNEL) staining were performed to visualize the surviving cells, ROS formation, and DNA fragmentation, respectively. Scale bar = 50 μm. All assays were performed in triplicate. Fluorescence intensities of 5-CFDA AM, DCF-DA, and TUNEL-stained cells were measured with an ELISA reader, and the data obtained were calibrated into percentile values versus the control group. Data are shown as mean ± standard deviation, and the differences were analyzed using one-way analysis of variance followed by Tukey's multiple comparison *post hoc* test ($^{a}p < 0.05$, significantly different from the control group; $^{b}p < 0.05$, significantly different from the vehicle group; $^{c}p < 0.05$, significantly different from the PFKFB3 group).

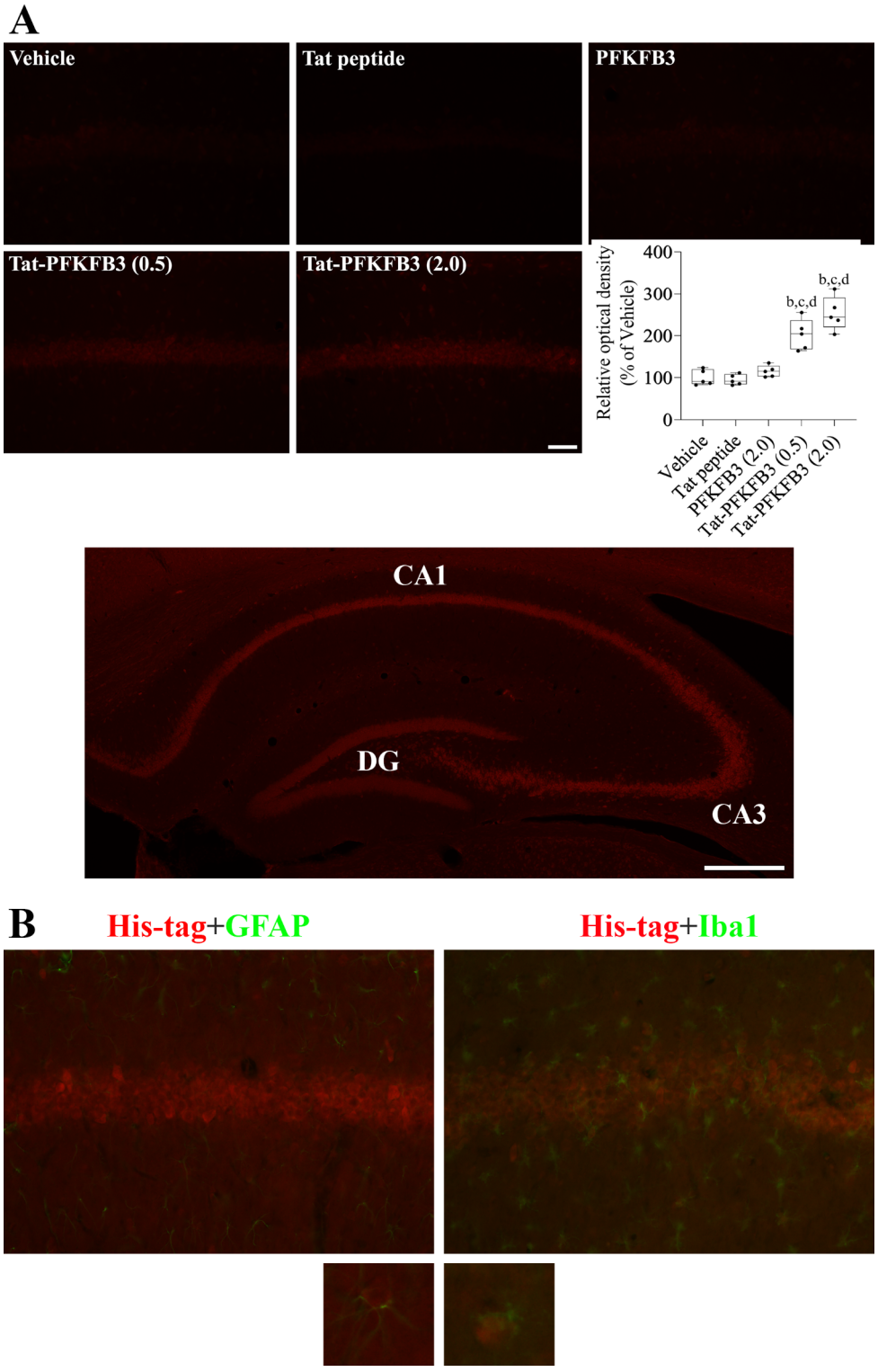

Fig. 3. Validation of synthesized Tat-PFKFB3 and PFKFB3 protein delivery in the gerbil hippocampus. (A) Immunohistochemical staining for His-tag was used to visualize intracellular delivery of PFKFB protein in the hippocampal CA1 region 2 h after ischemia. DG, dentate gyrus. (B) Double immunofluorescent histochemical staining for His-tag and GFAP or Iba1 was performed to visualize PFKFB delivery in astrocytes and microglia, respectively, 2 h after treatment with Tat-PFKFB3 and PFKFB3 protein. The images of the double immunostained cells are inserted as inset images. Scale bar = 50 μm and 400 (whole hippocampus). The fluorescence intensity of the His-tag was measured at the mid-point of the CA1 region. The obtained data were calibrated into percentile values compared to the control group. Data were analyzed using one-way analysis of variance followed by Tukey's multiple comparison *post hoc* test ($^{a}p < 0.05$, significantly different from the control group; $^{b}p < 0.05$, significantly different from the vehicle-treated group; $^{c}p < 0.05$, significantly different from the PFKFB3-treated group). Data are presented as mean ± standard deviation.

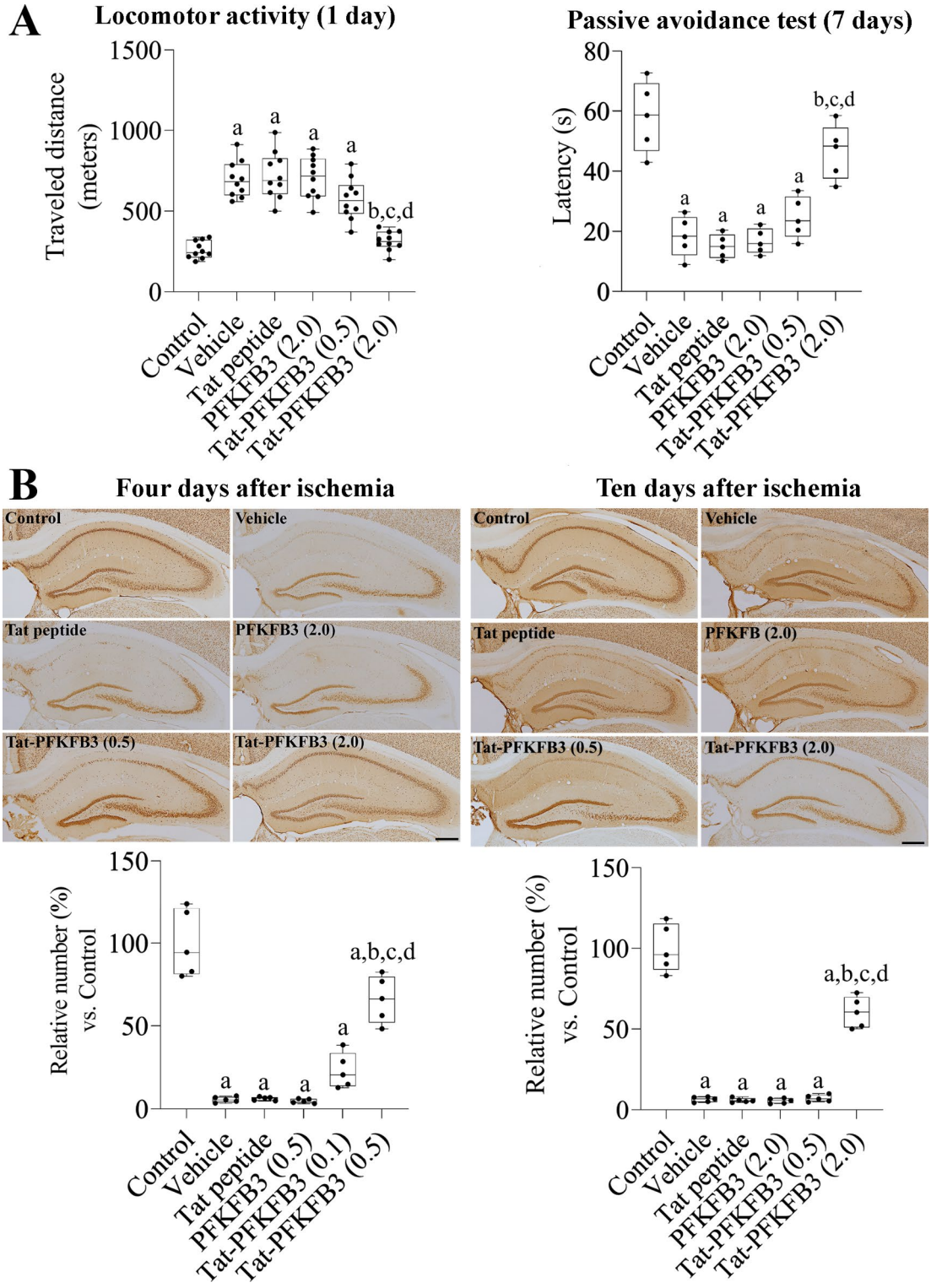

Fig. 4. Neuroprotective effects of Tat-PFKFB3 and PFKFB3 proteins on ischemia-induced neuronal damage in gerbils. (A) Locomotor activity was recorded, and the distance traveled was analyzed 24 h after ischemia to assess ischemia-induced hyperlocomotive activity. In addition, long-term memory deficits induced by ischemia were observed 7 days after ischemia via passive avoidance test. (B) Immunohistochemical staining for NeuN was performed to visualize the surviving neurons in the hippocampus 4 and 10 days after ischemia. Scale bar = 400 μm. The mid-point of the CA1 region was selected, and the number of NeuN-immunoreactive neurons was counted. The data obtained were calibrated into percentile values versus control group. Data were analyzed using one-way analysis of variance followed by Tukey's multiple comparison *post hoc* test ($^{a}p < 0.05$, significantly different from the control group; $^{b}p < 0.05$, significantly different from the vehicle-treated group; $^{c}p < 0.05$, significantly different from the PFKFB3-treated group). Data are presented as mean ± standard deviation.

latency was increased and significantly longer (79.9% of control) in the 2.0 mg/kg Tat-PFKFB3-treated group than that in the vehicle- or Tat peptide-treated groups (Fig. 4A).

Four and ten days after ischemia, surviving neurons were morphologically visualized via immunohistochemical staining for NeuN. In the control group, abundant NeuN-immunoreactive neurons were found in the hippocampal subregions, CA1-3, and the dentate gyrus. In the vehicle-, Tat peptide-, and 2.0 mg/kg PFKFB3-treated groups, NeuN-immunoreactive neurons were similarly detected in the hippocampus compared to that in the control group, except in the CA1 region, where a massive reduction of NeuN-immunoreactive neurons was observed. In these groups, the numbers of NeuN-immunoreactive neurons were 5.6%, 6.2%, and 4.7% in the CA1 region of the vehicle-, Tat peptide-, and 2.0 mg/kg PFKFB3-treated groups compared to those in the control group, respectively, 4 days after ischemia. Ten days after ischemia, the numbers decreased to 3.3%, 3.5%, and 3.5% in the CA1 region of the vehicle-, Tat peptide-, and 2.0 mg/kg PFKFB3-treated groups compared to those in the control group, respectively. In the 0.5 and 2.0 mg/kg Tat-PFKFB3-treated groups, more NeuN-immunoreactive neurons were found in the CA1 region, and their number significantly increased to 66.0% of that in the 2.0 mg/kg Tat-PFKFB3-treated group 4 days after ischemia. Ten days after ischemia, the number of NeuN-immunoreactive neurons was similar to that found in the 0.5 mg/kg Tat-PFKFB3-treated group compared to those in the vehicle-, Tat peptide-, or 2.0 mg/kg PFKFB3-treated groups. However, the number of NeuN-immunoreactive neurons was similar to that observed in the 2.0 mg/kg Tat-PFKFB3-treated group 4 and 10 days after ischemia (Fig. 4B).

The effect of Tat-PFKFB3 and PFKFB3 proteins on ischemia-induced Cdk5 expression in gerbils. Since PFKFB3 is closely associated with Cdk5, gerbils were sacrificed 24 h after ischemia. In the control group, Cdk5 immunoreactivity was observed in the cytoplasm of the CA1 and CA3 regions. In the vehicle-, Tat peptide-, and 2.0 mg/kg PFKFB3-treated groups, Cdk5 immunoreactivity was found in the cytosol of the CA3 region, while in the CA1 region, Cdk5 immunoreactivity was mainly observed in the nucleus. In contrast, in the 2.0 mg/kg Tat-PFKFB3-treated group, Cdk5 immunoreactivity was detected in the cytoplasm in the CA3 region and found in both the cytoplasm and nucleus in the CA1 region (Fig. 5A). To elucidate the increase in Cdk5 in the nuclear fraction, western blotting was performed using the nuclear fraction of hippocampal CA1 homogenates. Laminin B1, a nuclear envelope marker, was clearly observed in all lanes, but GAPDH, a cytoplasmic marker, was not detected. In the well-established nuclear fraction of the hippocampus, Cdk5 protein levels were significantly increased in the vehicle-, Tat peptide-, and 2.0 mg/kg PFKFB3-treated groups to 423.7%, 406.2%, and 418.7% of the control group, respectively. However, the increase in Cdk5 protein level in the nuclear fraction was significantly ameliorated in the 2.0 mg/kg Tat-PFKFB3-treated group, and the protein level was 230.9% of the control group (Fig. 5B).

Effects of Tat-PFKFB3 and PFKFB3 proteins on ROS formation in the hippocampal CA1 region. One day after ischemia/reperfusion, ROS formation was visualized by staining with DHE in the hippocampal CA1 region. In the control group, a very faint DHE fluorescence was observed in the hippocampal CA1 region. In the vehicle-, Tat peptide-, and 2.0 mg/kg PFKFB3-treated groups, DHE fluorescence was found in the stratum pyramidale of the CA1 region, and their optical densities were significantly increased to 310.3%, 317.8%, and 335.7% of the control group, respectively. In the 2.0 mg/kg Tat-PFKFB3-treated group, DHE fluorescence was detectable in the CA1 region, but the optical density was significantly decreased to 159.2% of the control group compared to the vehicle-, Tat peptide-, and 2.0 mg/kg PFKFB3-treated groups (Fig. 5C).

Discussion

Glycolysis is a compensatory mechanism that meets the energy needs of cells under various stress conditions[25,42–44]. Increased glycolysis has diverse cellular effects, increasing energy supply and inhibiting the production of ROS in cells[45–47]. PFKFB3 is a critical regulator of glycolysis, and its expression increases 12 h after oxygen and glucose deprivation[23]. In this study, we synthesized Tat-PFKFB3 to facilitate the intracellular delivery of PFKFB3 into HT22 cells, as the Tat peptide is considered a potential carrier of proteins and RNAs[48–50]. We observed an increase in Tat-PFKFB3 protein delivery in a concentration- and time-dependent manner based on western blotting and immunocytochemical staining for the His-tag; 6X His was added to the pET15b vector system. However, the control protein (PFKFB3) did not show a significant increase in the His-tag at any concentration or incubation time.

We investigated the effects of the Tat-PFKFB3 protein on H_2O_2-induced oxidative damage in HT22 cells and observed significant ameliorative effects on H_2O_2-induced neuronal death at concentrations of 6 μM and higher of Tat-PFKFB3 protein. We also observed a reduction in DNA fragmentation, ROS formation, and neuronal death in HT22 cells. This result is consistent with previous studies showing that pharmacological or genetic inhibition of PFKFB3 significantly alleviates pinocembrin-induced protective effects in cardiomyocytes[29] and increases sensitivity to Aβ toxicity[51]. However, pharmacological inhibition of PFKFB3 activity has shown neuroprotective effects against excitotoxic damage induced by NMDA, glutamate receptor activation, and oxygen-glucose deprivation[26]. A more recent study demonstrated that the accumulation of PFKFB3 in the cytosol causes neuronal death[52].

Thus, we expanded our observations to an in vivo ischemic model to assess the neuroprotective effects of Tat-PFKFB3 on hippocampal neurons. In previous studies, we noted the delivery of different Tat-fused proteins into the hippocampus[36,53,54]. In the present study, we assessed the delivery of PFKFB3 into the hippocampus through immunohistochemical staining for His-tag, and we observed intracellular localization of the His-tag. The transduced protein was predominantly observed in the neurons in the stratum pyramidale, while the delivery of Tat-PFKFB3 was found in the astrocytes and microglia. This result suggests that Tat-fused proteins could primarily be delivered to neurons, with a partial delivery to astrocytes and microglia. To elucidate the neuroprotective effects of Tat-PFKFB3 against ischemic damage, we examined spontaneous motor activity in gerbils 24 h after ischemia. This is because hyperlocomotive activity was observed before neuronal damage in the hippocampal CA1 region following ischemia in gerbils[55]. In contrast, passive avoidance was performed in this

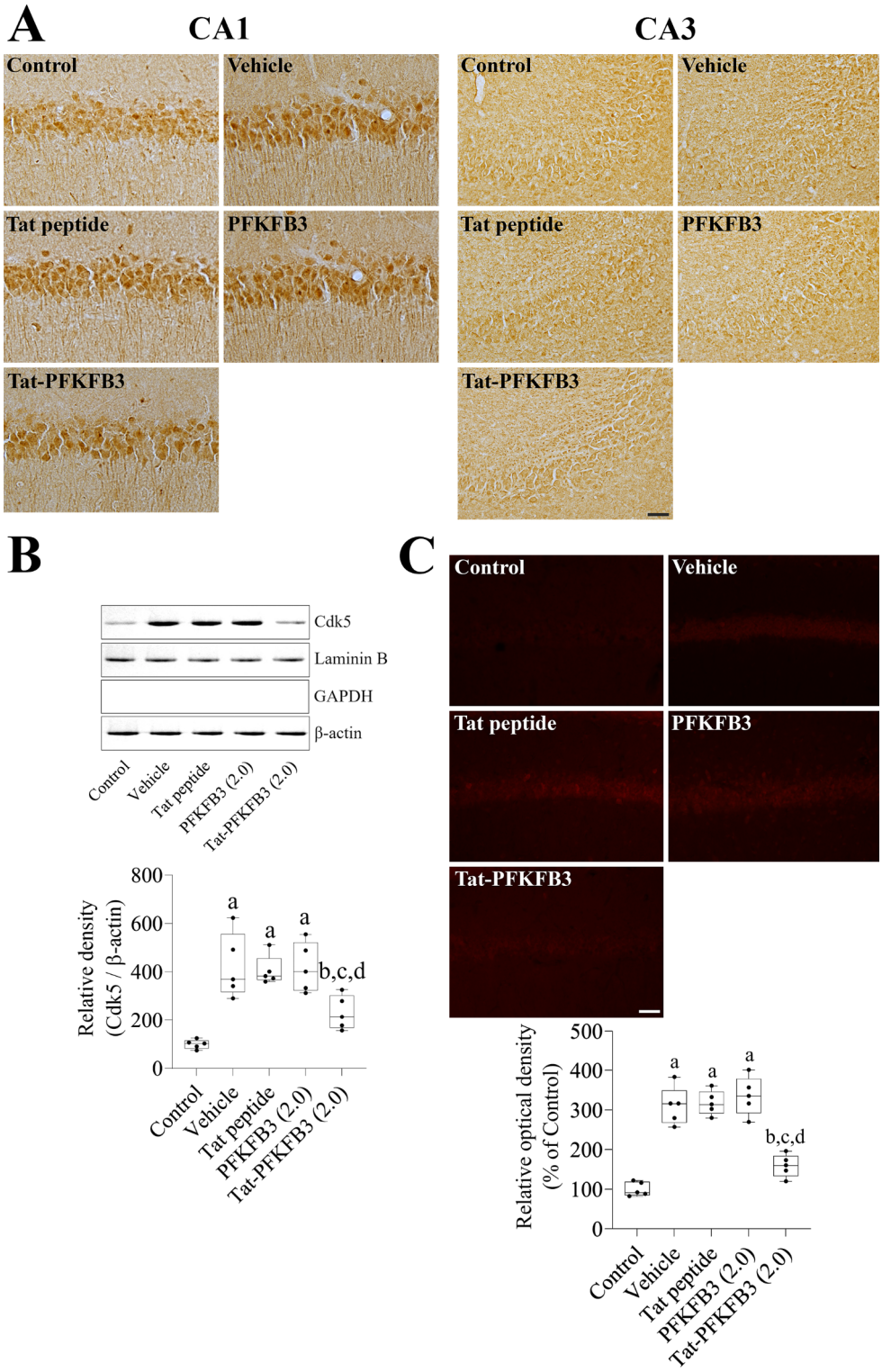

Fig. 5. Effect of Tat-PFKFB3 and PFKFB3 proteins on ischemia-induced Cdk5 expression and ROS formation in gerbils. (A) Immunohistochemical staining for Cdk5 was performed in the CA1 region 24 h after ischemia to assess the mechanisms of Tat-PFKFB3 and PFKFB3 against ischemia. Scale bar = 20 μm. (B) Western blotting for Cdk5 was conducted to change the protein levels in the nuclear fraction of hippocampal CA1 homogenates 24 h after ischemia. (C) DHE staining was used to visualize ROS formation in the hippocampal CA1 region 24 h after ischemia. The mid-point of the CA1 region was selected, and the DHE fluorescence intensity was measured. The data obtained were calibrated into percentile values compared to the control group. Data were analyzed using one-way analysis of variance followed by Tukey's multiple comparison *post hoc* test ($^{a}p < 0.05$, significantly different from the control group; $^{b}p < 0.05$, significantly different from the vehicle-treated group; $^{c}p < 0.05$, significantly different from the PFKFB3-treated group). Data are presented as mean ± standard deviation.

study to assess long-term memory impairment after neuronal death. Treatment with Tat-PFKFB3 significantly mitigated ischemia-induced hyperactivity and deficits in long-term memory 24 h and 7 days after ischemia. Additionally, we examined the surviving neurons in the hippocampus 4 and 10 days after ischemia to confirm whether Tat-PFKFB3 protects or delays neuronal death. Tat-PFKFB3 ameliorated neuronal death induced by ischemia within 10 days after ischemia. This finding is consistent with a previous study showing that the activation of PFKFB3 ameliorates neuronal damage induced by traumatic spinal cord injury, while PFKFB3 knockdown aggravates neuronal and white matter damage[28]. Other studies have also demonstrated that the pharmacological and genetic inhibition of PFKFB3 alleviates ischemia-induced neuronal damage[26,27] and hypoxia-induced pulmonary hypertension[56].

To address these discrepancies in the effects of PFKFB3, we evaluated Cdk5 levels in the hippocampal CA1 region post-ischemia. PFKFB3 is rapidly degraded in neurons via ubiquitylation by the APC/C-Cdh1[16], while PFKFB3 is stable in astrocytes due to low levels of APC/C-Cdh1[57]. However, PFKFB3 is stabilized when APC/C-Cdh1 is inhibited by Cdk5-p25[20,58] following overactivation of the NMDA receptors in neurons. Accumulation of PFKFB3 promotes glucose consumption, suppresses the PPP, and ultimately leads to neuronal death[21] due to the failure to maintain neuronal redox status through the PPP[59–61]. Moreover, Cdh1 overexpression has been shown to have neuroprotective effects against transient global cerebral ischemia and oxygen-glucose deprivation[23,62]. In this study, we observed Cdk5 immunoreactivity in the hippocampal CA1 region 24 h after ischemia, as it was significantly increased in the nuclear fraction at this time point[63]. Cdk5 immunoreactivity was detected in the nucleus 24 h after ischemia, when the protein level was significantly elevated in the hippocampal CA1 fraction. However, treatment with Tat-PFKFB3 significantly reduced Cdk5 protein levels in the nuclear fraction 24 h after ischemia. This suggests that treatment with Tat-PFKFB3 decreases Cdk5 expression in the nucleus, which may increase APC/C-Cdh1 levels in the hippocampus and attenuate ischemia-induced neuronal death. Nonetheless, this study had limitations. Several studies have proven that inhibiting Cdk5 either pharmacologically or genetically has potential neuroprotective effects against neuronal death in cases of focal cerebral ischemia[64,65] and oxygen-glucose deprivation[66]. Additionally, the Tat-PFKFB3 treatment significantly reduced the ischemia-induced production of ROS in the hippocampal CA1 region, as observed through DHE staining. However, in this study, we were unable to explain the discrepancy in the results. A recent study demonstrated that overexpression of PFKFB3 leads to an increase in mitochondrial ROS and impairs mitochondrial bioenergetics[67]. The time window is considered one of the most critical points in which continuous activation of PFKFB3 or pharmacological activation may cause neuronal damage by reducing the redox ability of neurons. However, in this study, we used exogenous PFKFB3, which may have acted through different mechanisms. The distinct roles of endogenous and exogenous PFKFB3 remain unclear. Additionally, although we administered Tat-PFKFB3 immediately after ischemia, the potential clinical relevance of delayed Tat-PFKFB3 treatment in ischemia treatment needs further elucidation.

Our study revealed that cell-permeable Tat-PFKFB3 can protect neurons from oxidative stress in HT22 cells and ischemic damage in the gerbil hippocampus. These beneficial effects of Tat-PFKFB3 may be associated with its inhibitory effect on Cdk5 translocation into the nucleus and its ability to reduce ROS formation. Therefore, Tat-PFKFB3 may be applicable for reducing neurological disorders associated with Cdk5.

Data availability

The datasets and supporting materials generated and/or analyzed during the current study are available from the corresponding author upon reasonable request.

Received: 21 June 2024; Accepted: 1 October 2024
Published online: 21 October 2024

References

1. Siegel, G. J. & Albers, R. W. *Basic Neurochemistry: Molecular, Cellular, and Medical Aspects* (Raven, 1994).
2. Dirnagl, U., Iadecola, C. & Moskowitz, M. A. Pathobiology of ischaemic stroke: an integrated view. *Trends Neurosci.* **22**, 391–397 (1999).
3. Lipton, P. Ischemic cell death in brain neurons. *Physiol. Rev.* **79**, 1431–1568 (1999).
4. Sims, N. R. & Muyderman, H. Mitochondria, oxidative metabolism and cell death in stroke. *Biochim. Biophys. Acta.* **1802**, 80–91 (2010).
5. Yatsu, F. M., Lee, L. W. & Liao, C. L. Energy metabolism during brain ischemia. Stability during reversible and irreversible damage. *Stroke.* **6**, 678–683 (1975).
6. Cao, B. Q., Tan, F., Zhan, J. & Lai, P. H. Mechanism underlying treatment of ischemic stroke using acupuncture: transmission and regulation. *Neural Regen Res.* **16**, 944–954 (2021).
7. León-Moreno, L. C., Castañeda-Arellano, R., Rivas-Carrillo, J. D. & Dueñas-Jiménez, S. H. Challenges and improvements of developing an ischemia mouse model through bilateral common carotid artery occlusion. *J. Stroke Cerebrovasc. Dis.* **29**, 104773 (2020).
8. Wang, Y. et al. Generation of gene-knockout Mongolian gerbils via CRISPR/Cas9 system. *Front. Bioeng. Biotechnol.* **8**, 780 (2020).
9. Zorio, D. A. R. et al. De novo sequencing and initial annotation of the Mongolian gerbil (Meriones unguiculatus) genome. *Genomics.* **111**, 441–449 (2019).
10. Ahn, J. H. et al. Differential regional infarction, neuronal loss and gliosis in the gerbil cerebral hemisphere following 30 min of unilateral common carotid artery occlusion. *Metab. Brain Dis.* **34**, 223–233 (2019).
11. Kawalec, M. et al. Mitochondrial dynamics, elimination and biogenesis during post-ischemic recovery in ischemia-resistant and ischemia-vulnerable gerbil hippocampal regions. *Biochim. Biophys. Acta Mol. Basis Dis.* **1869**, 166633 (2023).
12. Lee, C. H. et al. Relationship between neuronal damage/death and astrogliosis in the cerebral motor cortex of gerbil models of mild and severe ischemia and reperfusion injury. *Int. J. Mol. Sci.* **23**, 5096 (2022).
13. Shiino, A., Matsuda, M., Handa, J. & Chance, B. Poor recovery of mitochondrial redox state in CA1 after transient forebrain ischemia in gerbils. *Stroke.* **29**, 2421–2424 (1998). discussion 2425.

14. Rider, M. H. et al. 6-phosphofructo-2-kinase/fructose-2,6-bisphosphatase: head-to-head with a bifunctional enzyme that controls glycolysis. *Biochem. J.* **381**, 561–579 (2004).
15. Fagerberg, L. et al. Analysis of the human tissue-specific expression by genome-wide integration of transcriptomics and antibody-based proteomics. *Mol. Cell. Proteom.* **13**, 397–406 (2014).
16. Herrero-Mendez, A. et al. The bioenergetic and antioxidant status of neurons is controlled by continuous degradation of a key glycolytic enzyme by APC/C-Cdh1. *Nat. Cell. Biol.* **11**, 747–752 (2009).
17. Almeida, A. Regulation of APC/C-Cdh1 and its function in neuronal survival. *Mol. Neurobiol.* **46**, 547–554 (2012).
18. Bolaños, J. P. Bioenergetics and redox adaptations of astrocytes to neuronal activity. *J. Neurochem.* **139** (Suppl 2), 115–125 (2016).
19. Tu, D. et al. The pentose phosphate pathway regulates chronic neuroinflammation and dopaminergic neurodegeneration. *J. Neuroinflammation*. **16**, 255 (2019).
20. Maestre, C., Delgado-Esteban, M., Gomez-Sanchez, J. C., Bolaños, J. P. & Almeida, A. Cdk5 phosphorylates Cdh1 and modulates cyclin B1 stability in excitotoxicity. *EMBO J.* **27**, 2736–2745 (2008).
21. Rodriguez-Rodriguez, P., Fernandez, E., Almeida, A. & Bolaños, J. P. Excitotoxic stimulus stabilizes PFKFB3 causing pentose-phosphate pathway to glycolysis switch and neurodegeneration. *Cell. Death Differ.* **19**, 1582–1589 (2012).
22. de Veas-Pérez, M. et al. Regulation of Bcl-xL-ATP synthase interaction by mitochondrial cyclin B1-cyclin-dependent kinase-1 determines neuronal survival. *J. Neurosci.* **35**, 9287–9301 (2015).
23. Li, Z. et al. APC-Cdh1 regulates neuronal apoptosis through modulating glycolysis and pentose-phosphate pathway after oxygen-glucose deprivation and reperfusion. *Cell. Mol. Neurobiol.* **39**, 123–135 (2019).
24. Li, H. et al. Neurons require glucose uptake and glycolysis in vivo. *Cell. Rep.* **42**, 112335 (2023).
25. Lv, Y. et al. PFKFB3-mediated glycolysis is involved in reactive astrocyte proliferation after oxygen-glucose deprivation/reperfusion and is regulated by Cdh1. *Neurochem Int.* **91**, 26–33 (2015).
26. Burmistrova, O. et al. Targeting PFKFB3 alleviates cerebral ischemia-reperfusion injury in mice. *Sci. Rep.* **9**, 11670 (2019).
27. Yan, J. et al. Glycolysis inhibition ameliorates brain injury after ischemic stroke by promoting the function of myeloid-derived suppressor cells. *Pharmacol. Res.* **179**, 106208 (2022).
28. Gao, L. et al. 6-phosphofructo-2-kinase/fructose-2,6-bisphosphatase suppresses neuronal apoptosis by increasing glycolysis and cyclin-dependent kinase 1-mediated phosphorylation of p27 after traumatic spinal cord injury in rats. *Cell. Transpl.* **29**, 963689720950226 (2020).
29. Zheng, Y., Wan, G., Yang, B., Gu, X. & Lin, J. Cardioprotective natural compound pinocembrin attenuates acute ischemic myocardial injury via enhancing glycolysis. *Oxid. Med. Cell. Longev.* 4850328 (2020). (2020).
30. Sakamuri, S. S. et al. Aging related impairment of brain microvascular bioenergetics involves oxidative phosphorylation and glycolytic pathways. *J. Cereb. Blood Flow. Metab.* **42**, 1410–1424 (2022).
31. Ryan, T. E. et al. PFKFB3-mediated glycolysis rescues myopathic outcomes in the ischemic limb. *JCI Insight*. **5**, e139628 (2020).
32. Luo, J. et al. Cardiac-specific PFKFB3 overexpression prevents diabetic cardiomyopathy via enhancing OPA1 stabilization mediated by K6-linked ubiquitination. *Cell. Mol. Life Sci.* **81**, 228 (2024).
33. Yuan, Y., Sun, J., Dong, Q. & Cui, M. Blood-brain barrier endothelial cells in neurodegenerative diseases: signals from the barrier. *Front. Neurosci.* **17**, 1047778 (2023).
34. Parrasia, S., Szabò, I., Zoratti, M. & Biasutto, L. Peptides as pharmacological carriers to the brain: promises, shortcomings and challenges. *Mol. Pharm.* **19**, 3700–3729 (2022).
35. Hahn, K. R., Kwon, H. J., Yoon, Y. S., Kim, D. W. & Hwang, I. K. CHIP ameliorates neuronal damage in H_2O_2-induced oxidative stress in HT22 cells and gerbil ischemia. *Sci. Rep.* **12**, 20659 (2022).
36. Kwon, H. J. et al. Tat-malate dehydrogenase fusion protein protects neurons from oxidative and ischemic damage by reduction of reactive oxygen species and modulation of glutathione redox system. *Sci. Rep.* **13**, 5653 (2023).
37. Alonso-Alonso, M. L. et al. Need for a paradigm shift in the treatment of ischemic stroke: the blood-brain barrier. *Int. J. Mol. Sci.* **23**, 9486 (2022).
38. Long, Y. et al. Brain targeted borneol-baicalin liposome improves blood-brain barrier integrity after cerebral ischemia-reperfusion injury via inhibiting HIF-1α/VEGF/eNOS/NO signal pathway. *Biomed. Pharmacother.* **160**, 114240 (2023).
39. Al Shoyaib, A., Archie, S. R. & Karamyan, V. T. Intraperitoneal route of drug administration: should it be used in experimental animal studies? *Pharm. Res.* **37**, 12 (2019).
40. Radtke-Schuller, S. et al. Brain atlas of the Mongolian gerbil (*Meriones unguiculatus*) in CT/MRI-aided stereotaxic coordinates. *Brain Struct. Funct.* **221** (Suppl 1), 1–272 (2016).
41. Jung, H. Y. et al. Extracts from *Dendropanax morbifera* leaves ameliorates cerebral ischemia-induced hippocampal damage by reducing oxidative damage in gerbil. *J. Stroke Cerebrovasc. Dis.* **33**, 107483 (2024).
42. Bolaños, J. P., Almeida, A. & Moncada, S. Glycolysis: a bioenergetic or a survival pathway? *Trends Biochem. Sci.* **35**, 145–149 (2010).
43. Carpenter, K. L., Jalloh, I. & Hutchinson, P. J. Glycolysis and the significance of lactate in traumatic brain injury. *Front. Neurosci.* **9**, 112 (2015).
44. Geng, J. et al. Metabolomic profiling reveals that reprogramming of cerebral glucose metabolism is involved in ischemic preconditioning-induced neuroprotection in a rodent model of ischemic stroke. *J. Proteome Res.* **18**, 57–68 (2019).
45. Archer, S. L. Acquired mitochondrial abnormalities, including epigenetic inhibition of superoxide dismutase 2, in pulmonary hypertension and cancer: therapeutic implications. *Adv. Exp. Med. Biol.* **903**, 29–53 (2016).
46. Doménech, E. et al. AMPK and PFKFB3 mediate glycolysis and survival in response to mitophagy during mitotic arrest. *Nat. Cell. Biol.* **17**, 1304–1316 (2015).
47. Gottlob, K. et al. Inhibition of early apoptotic events by Akt/PKB is dependent on the first committed step of glycolysis and mitochondrial hexokinase. *Genes Dev.* **15**, 1406–1418 (2001).
48. Ansari, M. A. et al. State-of-the-art tools to elucidate the therapeutic potential of TAT-peptide (TP) conjugated repurposing drug against SARS-CoV-2 spike glycoproteins. *Curr. Pharm. Des.* **28**, 3706–3719 (2022).
49. Nakamura, M., Fujiwara, K. & Doi, N. Cytoplasmic delivery of siRNA using human-derived membrane penetration-enhancing peptide. *J. Nanobiotechnol.* **20**, 458 (2022).
50. Pei, D. How do biomolecules cross the cell membrane? *Acc. Chem. Res.* **55**, 309–318 (2022).
51. Lopez-Fabuel, I. et al. Aberrant upregulation of the glycolytic enzyme PFKFB3 in CLN7 neuronal ceroid lipofuscinosis. *Nat. Commun.* **13**, 536 (2022).
52. Ahmad, I. et al. Exploring the role of glycolytic enzymes PFKFB3 and GAPDH in the modulation of Aβ and neurodegeneration and their potential of therapeutic targets in Alzheimer's disease. *Appl. Biochem. Biotechnol.* **195**, 4673–4688 (2023).
53. Kaiafas, G. C. et al. *In vivo* biodistribution study of TAT-L-Sco2 fusion protein, developed as protein therapeutic for mitochondrial disorders attributed to *SCO2* mutations. *Mol. Genet. Metab. Rep.* **25**, 100683 (2020).
54. Kim, W. et al. P27 protects neurons from ischemic damage by suppressing oxidative stress and increasing autophagy in the hippocampus. *Int. J. Mol. Sci.* **21**, 9496 (2020).
55. Karasawa, Y., Araki, H. & Otomo, S. Changes in locomotor activity and passive avoidance task performance induced by cerebral ischemia in Mongolian gerbils. *Stroke*. **25**, 645–650 (1994).
56. Wang, L. et al. Mice with a specific deficiency of Pfkfb3 in myeloid cells are protected from hypoxia-induced pulmonary hypertension. *Br. J. Pharmacol.* **178**, 1055–1072 (2021).
57. Ippati, S. et al. Rapid initiation of cell cycle reentry processes protects neurons from amyloid-β toxicity. *Proc. Natl. Acad. Sci. U.S.A.* 118, e2011876118 (2021).

58. Lapresa, R., Agulla, J., Gonzalez-Guerrero, S., Bolaños, J. P. & Almeida, A. Amyloid-β induces Cdh1-mediated Rock2 stabilization causing neurodegeneration. *Front. Pharmacol.* **13**, 884470 (2022).
59. Delgado-Esteban, M., Almeida, A. & Bolaños, J. P. D-Glucose prevents glutathione oxidation and mitochondrial damage after glutamate receptor stimulation in rat cortical primary neurons. *J. Neurochem.* **75**, 1618–1624 (2000).
60. García-Nogales, P., Almeida, A. & Bolaños, J. P. Peroxynitrite protects neurons against nitric oxide-mediated apoptosis. A key role for glucose-6-phosphate dehydrogenase activity in neuroprotection. *J. Biol. Chem.* **278**, 864–874 (2003).
61. Rodriguez-Rodriguez, P., Fernandez, E. & Bolaños, J. P. Underestimation of the pentose-phosphate pathway in intact primary neurons as revealed by metabolic flux analysis. *J. Cereb. Blood Flow. Metab.* **33**, 1843–1845 (2013).
62. Zhang, J. et al. Protein kinase D3 promotes gastric cancer development through p65/6-phosphofructo-2-kinase/fructose-2,6-biphosphatase 3 activation of glycolysis. *Exp. Cell. Res.* **380**, 188–197 (2019).
63. Shin, B. N. et al. Down-regulation of cyclin-dependent kinase 5 attenuates p53-dependent apoptosis of hippocampal CA1 pyramidal neurons following transient cerebral ischemia. *Sci. Rep.* **9**, 13032 (2019).
64. Menn, B. et al. Delayed treatment with systemic (S)-roscovitine provides neuroprotection and inhibits in vivo CDK5 activity increase in animal stroke models. *PLoS One*. **5**, e12117 (2010).
65. Wen, Y. et al. Cdk5 is involved in NFT-like tauopathy induced by transient cerebral ischemia in female rats. *Biochim. Biophys. Acta*. **1772**, 473–483 (2007).
66. Chen, C. et al. CDK5 inhibition protects against OGDR induced mitochondrial fragmentation and apoptosis through regulation of Drp1S616 phosphorylation. *Life Sci.* **269**, 119062 (2021).
67. Jimenez-Blasco, D. et al. Weak neuronal glycolysis sustains cognition and organismal fitness. *Nat. Metab.* **6**, 1253–1267 (2024).

Author contributions

H. J. K., K.R.H., S.M.M., D.Y.Y., D.W.K, and I.K.H. conceived the study. H. J. K., K.R.H., D. W. K., and I.K.H. designed the study and prepared the manuscript. H.J.K., S.M.M., D. Y. Y., and I. K. H. conducted the animal experiments. H.J.K. and D.W.K. conducted biochemical experiments. H. J. K. and K.R.H. analyzed the data, and S.M.M. and D.Y.Y. participated in discussions of the study. All authors read and approved the manuscript, all data were generated in-house, and no paper mill was used.

Funding sources

This work was supported by Basic Science Research Program through the National Research Foundation of Korea (NRF) funded by the Korea government (MSIT) (NRF-2022R1A2B5B01002280 to In Koo Hwang and NRF-2021R1F1A1048079 to Dae Won Kim). In addition, this work was supported by the Research Institute for Veterinary Science, Seoul National University.

Declarations

Competing interests

The authors declare no competing interests.

Conflict of interest

The authors declare that there is no financial conflict of interests to publish these results.

Additional information

Supplementary Information The online version contains supplementary material available at https://doi.org/10.1038/s41598-024-75031-x.

Correspondence and requests for materials should be addressed to D.W.K. or I.K.H.